JOC The Journal of Organic Chemistry

UNIVERSITY OF BIRMINGHAM

Subscriber access provided by University of Birmingham

Article

Visible Light-Induced Oxidative Cross Dehydrogenative Coupling of Glycine Esters with #-Naphthols: Access to 1,3-Benzoxazines

Yuan Zhang, Shilin Li, Yin Zhu, Xiaorong Yang, Huang Zhou, and Ying Li

J. Org. Chem., **Just Accepted Manuscript** • DOI: 10.1021/acs.joc.9b01440 • Publication Date (Web): 13 Apr 2020

Just Accepted

is published by the American Chemical Society. 1155 Sixteenth Street N.W., Washington, DC 20036

Visible Light-Induced Oxidative Cross Dehydrogenative Coupling of Glycine Esters with β-Naphthols: Access to 1,3-Benzoxazines

Yuan Zhang*, Shilin Li, Yin Zhu, Xiaorong Yang, Huang Zhou, and Ying Li*

State Key Laboratory of Applied Organic Chemistry, College of Chemistry and Chemical Engineering, Lanzhou University, Lanzhou 730000, People's Republic of China

E-mail: zhangyuan@lzu.edu.cn; liying@lzu.edu.cn.

Abstract:

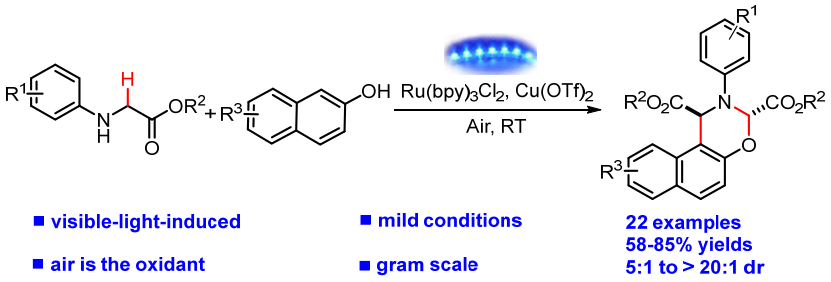

A direct aerobic oxidative dehydrogenative coupling reaction of glycine esters with β-naphthols has been achieved via the synergistic combination of photoredox catalysis and Lewis acid catalysis. A wide range of glycine esters and β-naphthols are suitable substrates for this reaction. A variety of 1,3-benzoxazines were obtained in good yields and excellent diastereoselectivities under mild reaction conditions. Moreover, this protocol could be performed on gram-scale, without considerable loss in activity.

Introduction

The 1,3-benzoxazine skeletons are privileged structural units that exist widely in pharmaceutically active molecules, which typically exhibit a variety of biological activities, such as antitumor,[1] antibacterial[2] and anti-HIV activities;[3] some 1,3-naphthoxazine derivatives show potential application prospect for the treatment of Parkinson's disease.[4] Moreover, these structure motifs also serve as important synthetic intermediates for the synthesis of bioactive natural products[5] and thermosetting polymers.[6] Consequently, this privileged structure has attracted great

interest from synthetic chemists.[7] Despite remarkable advances have been made, searching for more step-economic and green transformations to construct 1,3-benzoxazines is still in great demand.

On the other hand, the oxidative cross dehydrogenative coupling (CDC) reaction, which avoids the tedious prefunctionalization of the starting materials, has emerged as one of the most straightforward and atom-economical approaches for constructing carbon-carbon and carbon-heteroatom bonds.[8] Among these reactions, the oxidation of C_{sp3}–H bonds adjacent to a nitrogen atom has been regarded as one of the most important and useful strategies for C_{sp3}–H functionalization.[9] Pioneering works from the group of Xiao[10a] and Maycock[10b] have led to impressive synthesis of 1,3-benzoxazines via intramolecular oxidative dehydrogenative coupling of tertiary heterocyclic amines. Inspired by this strategy, several groups, including those of Jana,[10c] Maiti,[10d] Deb and Baruah,[10e-10g] and others,[10h-10k] have developed various catalytic systems for the synthesis of 1,3-benzoxazines via similar intramolecular CDC reactions (Scheme 1, a). In contrast, however, the synthesis of 1,3- benzoxazines via an intermolecular CDC reaction employing secondary amines (e.g. glycine derivatives) as substrates is still not easily accessible.[11]

Glycine derivatives are cheap and abundant starting materials in organic synthesis. Since the original work of Li,[12] the direct oxidative dehydrogenative coupling of glycine derivatives with various nucleophiles have emerged as an efficient approach for the straightfoward synthesis of α-amino acid derivatives[13] and azo-heterocyclic compounds.[14] However, most of these protocols typically need stoichiometric amounts of sacrificial oxidants to complete the transformation, thereby leading to toxic waste byproducts and low atom economy; and some of them were carried out at harsh conditions. In this context, in the past few years, visible light-induced photoredox catalysis[15] has become a promising tool to trigger the CDC reaction, owing to its mild, clean, and environmentally benign charicteristics.[16-18] However, to date, most of the reported photoredox catalyzed CDC reactions have focused on the α-C_{sp3}–H functionalization of tertiary amines (i.e., tetrahydroisoquinolines),[16] whereas examples relating to the α-C_{sp3}–H functionalization of secondary amines, are rather scarce.[17]

Scheme 1. CDC Process for the Synthesis of 1,3-Benzoxazines

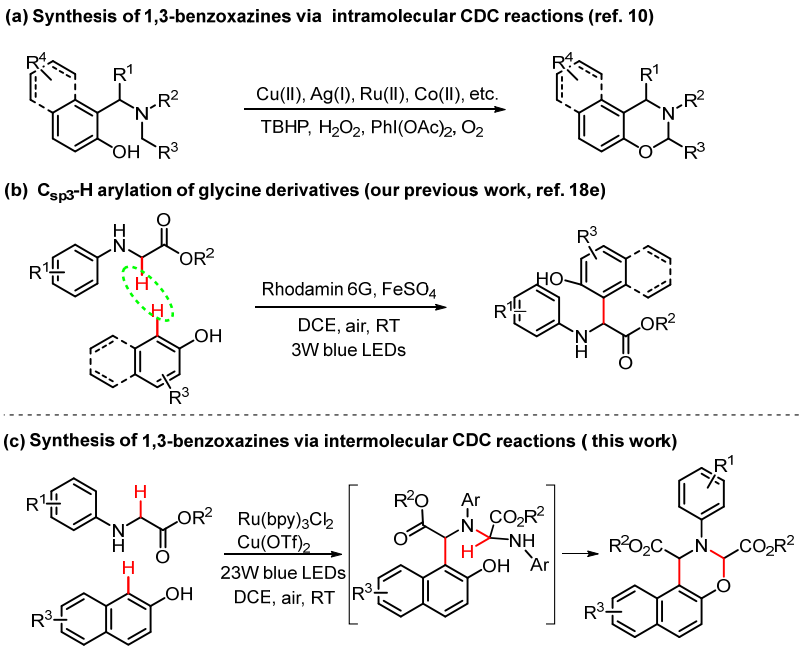

Our laboratory has a longstanding interest in the visible light-driven CDC reactions for the C_{sp3}-H functionalization of glycine derivatives.[18] In our recent study, we reported a visible light-induced oxidative cross-coupling reaction of glycine derivatives with phenols (Scheme 1, b).[18e] During the course of this reaction, we detected trace amount of 1,3-benzoxazines. Inspired by this observation, we hypothesized that whether these arylglycines could trap another equivalent of imine intermediate, thereby providing a new intermolecular CDC strategy for the synthesis of 1,3-benzoxazines (Scheme 1, c). Herein, we accordingly report a new photoredox catalytic aerobic oxidative dehydrogenative coupling/cyclization tandem reaction of glycine esters with β-naphthols for the efficient synthesis of 1,3-benzoxazines under mild conditions.

Results and Discussion

Our investigation into this new visible-light-induced protocol started with exposure of glycine ester **1a** and β-naphthol **2a** in the presence of Rhodamine 6G (Rh-6G)/$FeSO_4 \cdot 7H_2O$ in DCE under the irradiation of a 23 W blue LED strip (Table 1). We found that the addition sequence had an obvious influence for this reaction: under condition A (the standard condition of our previous work, as shown in Table 1)[18e], arylglycine **4aa** was isolated as the solely product, and only trace 1,3-benzoxazine **3aa** could be detected (Table 1, entry 1); Pleasingly, the targeted 1,3-benzoxazine**3aa** could be obtained in 15% yield under condition B (Table 1, entry 2). The increase of the amount of **1a** enhanced the yield of **3aa** to 22% (Table 1, entry 3). Notably, **3aa** was isolated as a single diastereomer. The relative configuration of **3aa** was established

unambiguously as trans by single-crystal X-ray diffraction analysis,[19] which may be attributed to the steric effects.

Table 1. Initial Studies [a]

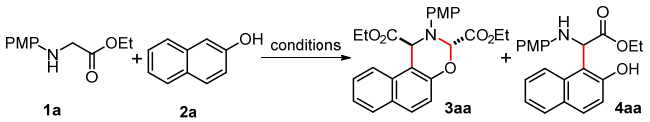

Entry	Condition	**3aa** Yield (%)[b]	**4aa** Yield (%)[b]
1	Condition A	trace	85
2	Condition B	15	74
3[c]	Condition B	22	69

[a] Condition A: **1a** (0.1 mmol), Rh-6G (2 mol %), $FeSO_4 \cdot 7H_2O$ (20 mol %), DCE (1.0 mL), 23 W blue LED light irradiation under air for 3 h at room temperature, then **2a** (0.12 mmol) was added, and stirred for another 3 h; Condition B: **1a** (0.1 mmol), **2a** (0.12 mmol), Rh-6G (2 mol %), $FeSO_4 \cdot 7H_2O$ (20 mol %), DCE (1.0 mL), 23 W blue LEDs light irradiation under air for 36 h at room temperature. [b] Yield of the isolated product, determined based on **1a**. [c] 0.25 mmol **1a** and 0.1 mmol **2a** were used, the yields of **3aa** and **4aa** were determined based on **2a**.

Encouraged by these initial results, we then conducted a series of screening studies for this protocol (Table 2, for details, see the Supporting Information). We first screened a variety of photocatalysts and Lewis acids (Table 2, entries 1−9). The results identified $Ru(bpy)_3Cl_2 \cdot 6H_2O/Cu(OTf)_2$ as the optimal catalyst combination, and **3aa** was obtained in 72% yield (Table 2, entry 4). It is worth noting that a variety of organic-dyes, such as Eosin Y, Rose Bengal and Rh-6G, are also capable photocatalysts for this transformation, though slight lower yields were provided (Table 2, entries 1−3). We also performed this reaction with Brønsted acid (e.g. HCl, TfOH), however, complicated products were obtained. Further evaluation of solvents revealed that DCE or toluene as the solvent were the best choices (Table 2, entries 10−14). A slight decrease of the concentration enhanced the formation of **3aa** in 76% yield (Table 2, entry 14). Notably, reducing the photocatalyst stoichiometry to 1 mol % and $Cu(OTf)_2$ stoichiometry to 10 mol % could be well tolerated, affording a good yield (79%) of the **3aa** (Table 2, entry 16). The byproduct of this reaction is the direct coupling product of **1a** with **2a** (compound **4aa**, 10% yield). Moreover, control experiments indicated that visible light, photocatalyst, acid, and air are all essential for this reaction (Table 2, entries 17−20).

Table 2. Optimization of Reaction Conditions[a]

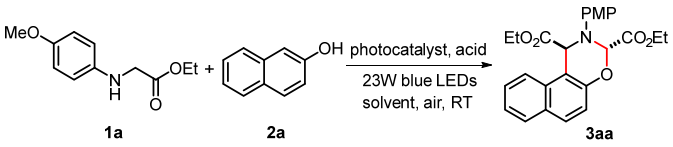

Entry	PC/ Acid	Solvent	Yield(%)[b]
1	Rh-6G/$Cu(OTf)_2$	DCE	58
2	Rose Bengal/$Cu(OTf)_2$	DCE	64
3	Eosin Y/$Cu(OTf)_2$	DCE	56
4	$Ru(bpy)_3Cl_2·6H_2O/Cu(OTf)_2$	DCE	72
5	$Ru(bpy)_3Cl_2·6H_2O/FeSO_4$	DCE	26
6	$Ru(bpy)_3Cl_2·6H_2O/CuSO_4$	DCE	66
7	$Ru(bpy)_3Cl_2·6H_2O$/CuCl	DCE	60
8	$Ru(bpy)_3Cl_2·6H_2O/CuBr_2$	DCE	65
9	$Ru(bpy)_3Cl_2·6H_2O/Zn(OTf)_2$	DCE	21
10	$Ru(bpy)_3Cl_2·6H_2O/Cu(OTf)_2$	MeOH	trace
11	$Ru(bpy)_3Cl_2·6H_2O/Cu(OTf)_2$	CH_3CN	67
12	$Ru(bpy)_3Cl_2·6H_2O/Cu(OTf)_2$	toluene	74
13	$Ru(bpy)_3Cl_2·6H_2O/Cu(OTf)_2$	EtOAc	63
14[c]	$Ru(bpy)_3Cl_2·6H_2O/Cu(OTf)_2$	DCE	76
15[c,d]	$Ru(bpy)_3Cl_2·6H_2O/Cu(OTf)_2$	DCE	76
16[c,d,e]	$Ru(bpy)_3Cl_2·6H_2O/Cu(OTf)_2$	DCE	79
17[f]	$Ru(bpy)_3Cl_2·6H_2O/Cu(OTf)_2$	DCE	trace
18	—/$Cu(OTf)_2$	DCE	trace
19	$Ru(bpy)_3Cl_2·6H_2O$/—	DCE	trace
20[g]	$Ru(bpy)_3Cl_2·6H_2O/Cu(OTf)_2$	DCE	trace

[a] Reaction conditions: **1a** (0.25 mmol), **2a** (0.10 mmol), photocatalyst (2 mol %), Lewis acid (20 mol %), solvent (2.0 mL), 23 W blue LEDs light irradiation under air for 36 h at room temperature. [b] Yield of the isolated product. [c] 3.0 mL DCE was used. [d] 1.0 mol % of $Ru(bpy)_3Cl_2·6H_2O$ was used. [e] 10 mol % of $Cu(OTf)_2$ was used. [f] Reaction was carried out in the dark. [g] Reaction was carried out under nitrogen.

With the optimized reaction conditions in hand, we next examined the substrate scope of this visible-light-induced oxidative cross-coupling reaction. We first evaluated the glycine ester component. As shown in Table 3, the reaction proceeded smoothly with a range of glycine esters possessing various electron-donating substituted groups in the para-, ortho- or meta-positions at the benzene rings, giving the corresponding 1,3-benzoxazines in good yields. In general,

substrates with electron-rich aryl groups exhibited higher reactivities than those with electron-deficient aryl groups, probably due to the increase in nucleophilicity of the nitrogen. However, glycine esters bearing electron-withdrawing groups (i.e., halogen and ester) at the benzene rings failed to give the corresponding products. This may be attributed to the decrease in nucleophilicity of the nitrogen. The scope of the ester fragment was also examined. A range of ester substrates, such as methyl ester, isopropyl ester, *t*-butyl ester, and benzyl ester, were also amenable to this reaction, affording the products **3ja–3ma** with 78−83% yields. We have also performed the reaction with other substrates, such as *N*-alkyl glycine ester and other α-amino compounds (e.g. ketones and nitriles), however, no reaction occurred (for details see Figure S1).

Table 3. Scope of the Glycine Ester Component[a,b]

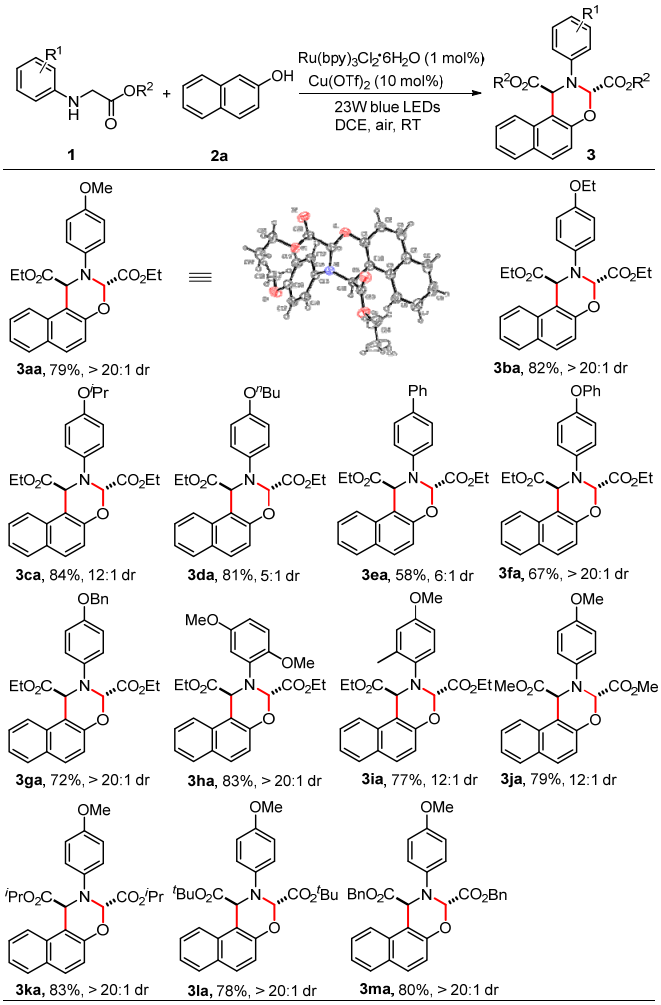

[a] Reaction conditions: **1** (0.25 mmol), **2a** (0.10 mmol), $Ru(bpy)_3Cl_2 \cdot 6H_2O$ (1 mol %), $Cu(OTf)_2$ (10 mol %), DCE (3.0 mL), 23 W blue LED light irradiation under air for 36 h at room temperature. [b] Yield of the isolated product, dr values were determined by ^1H NMR.

The substrate scope of β-naphthol component was subsequently investigated (Table 4). A variety of β-naphthols with both electron-donating and electron-withdrawing groups underwent the desired cross-coupling reaction smoothly, giving the corresponding products **3ab**−**3aj** in good yields (65−85%). Various functional groups such as ester, carboxyl, cyano and halogen are well tolerated in this transformation, which provide handles for further transformations. Moreover,

Table 4. Scope of the β-Naphthol Component[a,b]

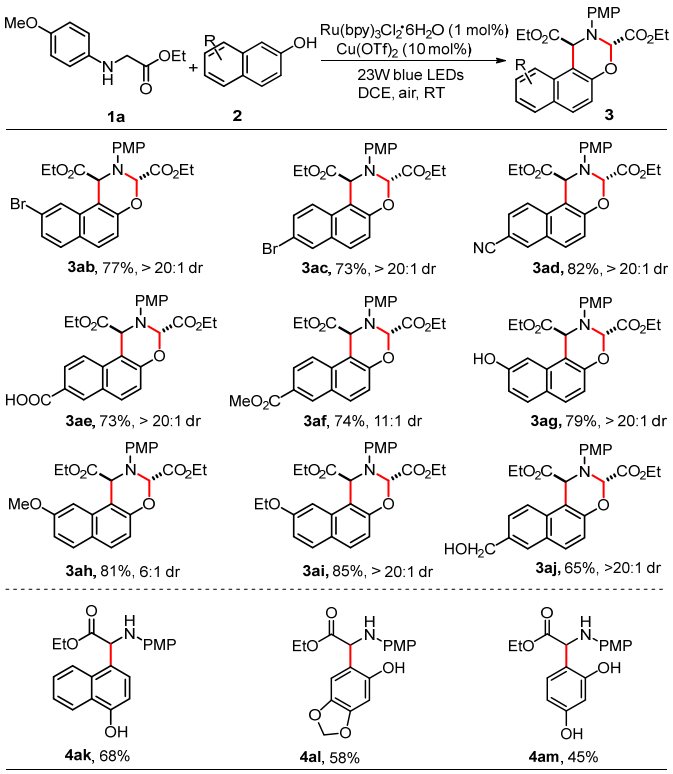

[a] Reaction conditions: **1a** (0.25 mmol), **2** (0.10 mmol), $Ru(bpy)_3Cl_2·6H_2O$ (1 mol %), $Cu(OTf)_2$ (10 mol %), DCE (3.0 mL), 23 W blue LED light irradiation under air for 36 h at room temperature. [b]Yield of the isolated product, dr values were determined by ^1H NMR.

besides β-naphthols, other electron-rich arenes, such as α-naphthol and phenols were also used as substrates, however, only arylglycines were obtained in these cases (**4ak**−**4am**). When α-naphthol was used as the substrate, CDC reaction occurred at the para-position of the hydroxyl group, so the coupling product **4ak** could not participate in the subsequent cyclization. When phenols were used as the substrates, intramolecular hydrogen bonds would be formed between the hydrogen atom of hydroxyl group and the nitrogen atom, which may dramatically decrease the nucleophilicity of the nitrogen, thereby inhibiting the second catalytic process. For β-naphthols,

this type of intramolecular hydrogen bond could not be formed, because in the coupling product (e.g. **4aa**), the steric effect between α-H of naphthalene ring and ester group would make hydroxyl group far away from the nitrogen atom (the computational studies also support this point, Figure 1). However, other possible reasons for the lack of reactivity with phenols should not be fully excluded.

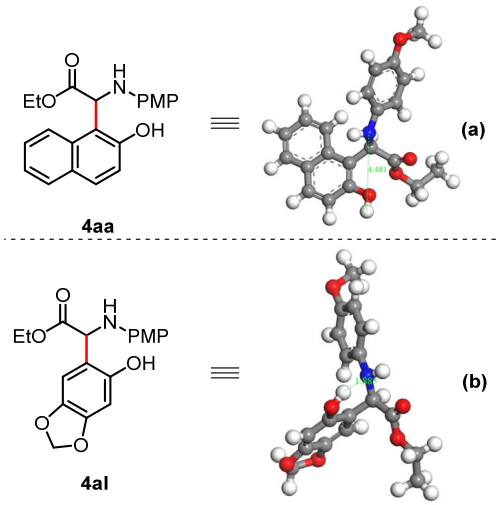

Figure 1. Computational Structures of Compounds **4aa** (a) and **4al** (b). In compound **4aa**, the distance between hydrogen atom of hydroxyl group and the nitrogen atom is ca 4.48 Å, indicating that intramolecular hydrogen bond could not be formed.

To evaluate the synthetic utility of this protocol, a gram-scale reaction of **1a** and **2a** (5 mmol) was conducted (Scheme 2a). The target product **3aa** was obtained in 74% yield. Furthermore, transformations of products were also conducted. As shown in Scheme 2b, the 1,3-benzoxazine ring was opened when treatment of **3aa** with NaOH, giving arylglycine **6** in 65% yield. We also tried the reduction of the ester groups by using $LiAlH_4$ as the reductant, however, a complicated mixture was obtained. Finally, the esterification of **3ae** with the bioactive podophyllotoxin **7** was successfully carried out in the presence of DMAP and DCC, affording the ester **8** in 72% yield (Scheme 2c).

Scheme 2. Gram-Scale Reactions of 1a and 2a and Transformations of the Products

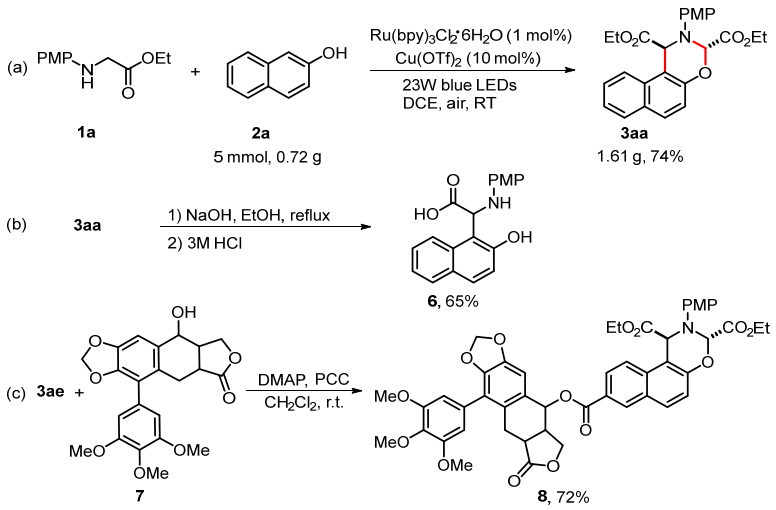

To provide insights about the reaction mechanisms of this transformations, a series of control experiments were conducted (Scheme 3). Firstly, when excessive TEMPO was subjected to the model reaction as a radical scavenger, only trace product could be observed (the TEMPO-trapped product **9** was identified by high-resolution mass spectrometry, see Figure S2), indicating that this reaction may include a radical process. Next, upon irradiation of **1a** with blue LEDs under the standard conditions, the imine intermediate **5a** was isolated in 86% yield. Thirdly, the obtained **5a** reacted readily with **2a** under the standard conditions, giving **3aa** in 90% yield. Finally, arylglycine **4aa** was synthesized[18e] and subjected to the standard reaction conditions, and product **3aa** was obtained in 94% yield; however, in the absence of photocatalyst, only trace **3aa** was observed. These results illustrated that **4aa** and **5a** should be key intermediates of this reaction.

Scheme 3. Control Experiments for Mechanistic Studies

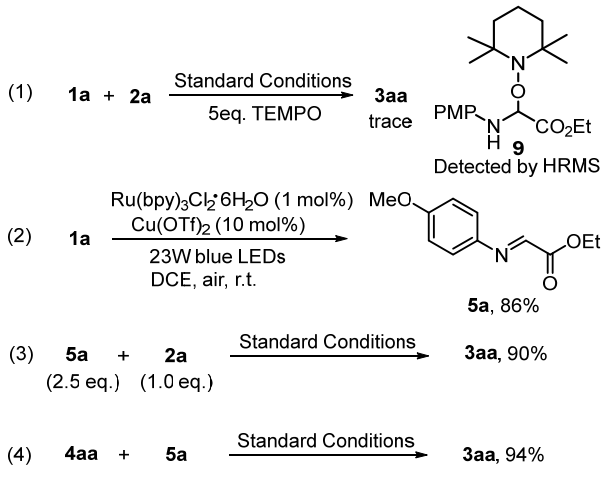

Scheme 4. Proposed Mechanism

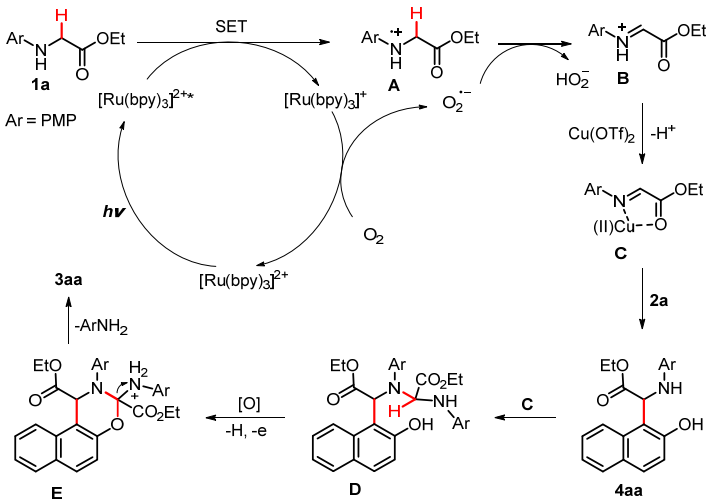

Based upon the above experimental results and precedent literatures, we proposed a possible mechanism for this photocatalytic oxidative dehydrogenative coupling reaction, as shown in Scheme 4. Firstly, the excited state $[Ru(bpy)_3]^{2+*}$ would accept a single electron from glycine ester **1a** to produce $[Ru(bpy)_3]^{+}$ and the radical cation **A**. The photocatalyst was then regenerated by the oxidation of O_2; an active species $O_2^{\bullet-}$ was formed during this process, which may abstract electron and proton from **A** to produce the iminium ion **B**. Next, the in situ generated HOO^- may abstract a proton from **B** to form the imine **5a**, which subsequently forms the active electrophile **C** under the influence of $Cu(OTf)_2$. Active intermediate **C** was then captured by β-naphthol **2a** to form arylglycine **4aa**, which further underwent intermolecular amination with intermediate **C** to afford intermediate **D**. Finally, a second oxidation of **D** and the sequential intramolecular nucleophilic attack and elimination of the aniline would afford the desired product **3aa**. The aniline byproduct could be detected by Thin-Layer Chromatography (TLC). Furthermore, acid catalyzed elimination of aniline from **D** to produce an iminium followed by cyclization is another alternative possible pathway. However, other possible mechanistic pathways should not be fully excluded. More details for the mechanism of this transform are currently under investigation.

Conclusion

In conclusion, we have realized a highly efficient aerobic oxidative dehydrogenative coupling reaction of glycine esters with β-naphthols via the synergistic combination of photoredox catalysis and Lewis acid catalysis. A range of 1,3-benzoxazine derivatives were obtained in good yields under mild reaction conditions. The potential synthetic value of this novel protocol was exemplified by gram-scale reactions. Further investigations toward an asymmetric variant of this

transform are currently underway in this laboratory.

Experimental Section

General Experimental Procedures

Unless otherwise noted, all reagents were purchased from commercial sources and used as received without further purification. Unless otherwise indicated, all experiments were carried out under air atmosphere. Irradiation of photochemical reactions was carried out using a 23 W blue LED strip. The silica gel (200-300 meshes) was used for column chromatography and TLC inspections were taken on silica gel GF254 plates. Liquid ^{1}H and ^{13}C NMR spectra were recorded on a 400 MHz spectrometer. The chemical shifts δ are given in ppm relative to tetramethylsilane and the coupling constants J are given in Hz. The spectra were recorded with $CDCl_3$ as solvent at room temperature. High resolution mass spectra (HRMS) were obtained on a mass spectrometer by using electrospray ionization (ESI) analyzed by quadrupole time-of-flight (QTof). *N*-arylglycine derivatives[13a,13b] were prepared according to literature procedures.

General Procedure for the Visible Light-Induced Oxidative Cross Dehydrogenative Coupling of Glycine Derivatives Esters with β-Naphthols.

A solution of *N*-arylglycine ester **1** (0.25 mmol, 2.5 eq), **2** (0.10 mmol, 1.0 eq), $Ru(bpy)_3Cl_2 \cdot 6H_2O$ (1 mol %, 0.001 mmol, 0.75 mg), $Cu(OTf)_2$ (10 mol %, 0.01 mmol, 3.6 mg) in dry DCE (3.0 mL) was irradiated with 23 W blue LED strip (400−500 nm) (at approximately 5 cm distance from the light source) under air atmosphere at room temperature for 36 h. After completion of the reaction as monitored by TLC, the solvent was concentrated in vacuo. The crude product was purified by flash chromatography on silica gel (petroleum ether/acetone = 8:1) to afford the products.

*Diethyl 2-(4-methoxyphenyl)-2,3-dihydro-1H-naphtho[1,2-e][1,3]oxazine-1,3-dicarboxylate (**3aa**).* Pale yellow oil (34.4 mg, 79% yield). ^{1}H NMR (400 MHz, $CDCl_3$) δ 7.79 (dd, J_1 = 8.4 Hz, J_2 = 4.5 Hz, 2H), 7.69 (d, J = 8.4 Hz, 1H), 7.51–7.44 (m, 1H), 7.41–7.35 (m, 1H), 7.34 (d, J = 9.0 Hz, 1H), 7.27–7.20 (m, 2H), 6.79–6.71 (m, 2H), 6.30 (s, 1H), 5.26 (s, 1H), 4.45–4.27 (m, 2H), 4.24–4.12 (m, 2H), 3.72 (s, 3H), 1.36 (t, J = 7.1 Hz, 3H), 1.12 (t, J = 7.1 Hz, 3H); ^{13}C {^{1}H}NMR (100

MHz, $CDCl_3$) δ 171.2, 166.1, 157.4, 151.8, 140.1, 131.2, 129.9, 129.5, 128.8, 127.1, 126.3, 124.0, 121.6, 119.1, 114.2, 110.4, 83.2, 63.7, 61.8, 61.7, 55.3, 14.1, 13.9; HRMS (ESI) calcd for $C_{25}H_{26}NO_6$ $(M+H)^+$ 436.1760, found 436.1762.

*Diethyl 2-(4-ethoxyphenyl)-2,3-dihydro-1H-naphtho[1,2-e][1,3]oxazine-1,3-dicarboxylate (**3ba**).* Pale yellow solid (36.9 mg, 82% yield), mp 68–69 °C. ^{1}H NMR (400 MHz, $CDCl_3$) δ 7.79 (dd, J_1 = 8.3 Hz, J_2 = 5.3 Hz, 2H), 7.68 (d, J = 8.4 Hz, 1H), 7.47 (t, J = 7.6 Hz, 1H), 7.42–7.30 (m, 2H), 7.22 (d, J = 8.9 Hz, 2H), 6.73 (d, J = 8.9 Hz, 2H), 6.29 (s, 1H), 5.26 (s, 1H), 4.45–4.26 (m, 2H), 4.25–4.10 (m, 2H), 3.94 (q, J = 7.0 Hz, 2H), 1.35 (t, J = 7.0 Hz, 6H), 1.12 (t, J = 7.1 Hz, 3H); ^{13}C {^{1}H}NMR (100 MHz, $CDCl_3$) δ 171.2, 166.1, 156.8, 151.9, 139.9, 131.3, 129.9, 129.5, 128.8, 127.1, 126.3, 124.0, 121.6, 119.2, 114.8, 110.5, 83.2, 63.7, 63.5, 61.8, 61.7, 14.7, 14.1, 13.9; HRMS (ESI) calcd for $C_{26}H_{28}NO_6$ $(M+H)^+$ 450.1917, found 450.1919.

*Diethyl 2-(4-isopropoxyphenyl)-2,3-dihydro-1H-naphtho[1,2-e][1,3]oxazine-1,3-dicarboxylate (**3ca**).* Pale yellow oil (38.9 mg, 84% yield). ^{1}H NMR (400 MHz, $CDCl_3$) δ 7.80 (dd, J_1 = 8.4 Hz, J_2 = 5.1 Hz, 2H), 7.70 (d, J = 8.3 Hz, 1H), 7.51–7.46 (m, 1H), 7.41–7.37 (m, 1H), 7.35 (d, J = 9.0 Hz, 1H), 7.27–7.16 (m, 2H), 6.78–6.70 (m, 2H), 6.31 (s, 1H), 5.28 (s, 1H), 4.46–4.37 (m, 2H), 4.35–4.31 (m, 1H), 4.27–4.12 (m, 2H), 1.36 (d, J = 7.2 Hz, 3H), 1.28 (dd, J_1 = 6.0 Hz, J_2 =3.7 Hz, 6H), 1.13 (t, J = 7.1 Hz, 3H); ^{13}C {^{1}H}NMR (100 MHz, $CDCl_3$) δ 171.2, 166.1, 155.7, 151.9, 139.9, 131.3, 129.9, 129.5, 128.8, 127.0, 126.3, 123.9, 121.6, 119.2, 116.2, 110.5, 83.2, 70.0, 63.7, 61.8, 61.7, 21.9, 21.8, 14.1, 13.8; HRMS (ESI) calcd for $C_{27}H_{30}NO_6$ $(M+H)^+$ 464.2073, found 464.2077.

*Diethyl 2-(4-butoxyphenyl)-2,3-dihydro-1H-naphtho[1,2-e][1,3]oxazine-1,3-dicarboxylate (**3da**).* Pale yellow oil (38.7 mg, 81% yield). ^{1}H NMR (400 MHz, $CDCl_3$) δ 7.79 (dd, J_1 = 8.4 Hz, J_2 = 5.0 Hz, 2H), 7.68 (d, J = 8.4 Hz, 1H), 7.47 (t, J = 7.2 Hz, 1H), 7.40–7.36 (m, 1H), 7.34 (d, J = 9.0 Hz, 1H), 7.25–7.18 (m, 2H), 6.74 (d, J = 8.9 Hz, 2H), 6.30 (s, 1H), 5.26 (s, 1H), 4.47–4.38 (m, 1H), 4.36– 4.26 (m, 1H), 4.25–4.12 (m, 2H), 3.86 (t, J = 6.5 Hz, 2H), 1.74–1.67 (m, 2H), 1.47–1.40 (m, 2H), 1.35 (t, J = 7.1 Hz, 3H), 1.12 (t, J = 7.1 Hz, 3H), 0.94 (t, J = 7.4 Hz, 3H); ^{13}C {^{1}H}NMR (100 MHz, $CDCl_3$) δ 171.2, 166.1, 156.9, 151.8, 139.9, 131.3, 129.9, 129.5, 128.8, 127.1, 126.3, 124.0, 123.6, 121.6, 119.2, 114.9, 114.8, 110.4, 83.2, 67.8, 63.8, 61.7, 61.6, 31.2, 19.1, 14.1, 13.9, 13.8. HRMS (ESI) calcd for $C_{28}H_{32}NO_6$ $(M+H)^+$ 478.2230, found 478.2235.

Diethyl 2-([1,1'-biphenyl]-4-yl)-2,3-dihydro-1H-naphtho[1,2-e][1,3]oxazine-1,3-dicarboxylate

*(**3ea**)*. Pale yellow solid (27.9 mg, 58% yield), mp 123–124 °C. ^{1}H NMR (400 MHz, $CDCl_3$) δ 7.80 (dd, J_1 = 8.4 Hz, J_2 = 3.9 Hz, 2H), 7.74 (d, J = 8.5 Hz, 1H), 7.52 (s, 1H), 7.51–7.47 (m, 3H), 7.46 (s, 1H), 7.43–7.36 (m, 6H), 7.35–7.31 (m, 1H), 6.38 (s, 1H), 5.49 (s, 1H), 4.44–4.33 (m, 2H), 4.28–4.19 (m, 2H), 1.38 (t, J = 7.1 Hz, 3H), 1.12 (t, J = 7.1 Hz, 3H); ^{13}C {^{1}H}NMR (100 MHz, $CDCl_3$) δ 171.1, 166.2, 151.8, 146.3, 140.4, 137.7, 131.2, 130.1, 129.6, 128.8, 128.7, 127.8, 127.2, 127.1, 126.8, 124.1, 123.5, 121.6, 119.1, 110.5, 82.6, 63.8, 61.9, 14.1, 13.8; HRMS (ESI) calcd for $C_{30}H_{28}NO_5$ $(M+H)^+$ 482.1967, found 482.1971.

*Diethyl 2-(4-phenoxyphenyl)-2,3-dihydro-1H-naphtho[1,2-e][1,3]oxazine-1,3-dicarboxylate (**3fa**)*. Pale red oil (33.3 mg, 67% yield). ^{1}H NMR (400 MHz, $CDCl_3$) δ 7.86–7.78 (m, 2H), 7.72 (d, J = 8.4 Hz, 1H), 7.53–7.49 (m, 1H), 7.44–7.38 (m, 1H), 7.36 (d, J = 9.0 Hz, 1H), 7.33–7.29 (m, 4H), 7.10–7.06 (m, 1H), 6.98–6.93 (m, 2H), 6.92–6.85 (m, 2H), 6.34 (s, 1H), 5.35 (s, 1H), 4.44–4.33 (m, 2H), 4.29–4.18 (m, 2H), 1.38 (t, J = 7.1 Hz, 3H), 1.16 (t, J = 7.1 Hz, 3H); ^{13}C {^{1}H}NMR (100 MHz, $CDCl_3$) δ 171.1, 165.9, 157.2, 154.6, 151.8, 142.5, 131.2, 130.1, 129.6, 129.5, 128.9, 127.1, 125.9, 124.1, 123.1, 121.6, 119.5, 119.1, 118.5, 110.3, 82.9, 63.8, 61.9, 61.8, 14.1, 13.9; HRMS (ESI) calcd for $C_{30}H_{28}NO_6$ $(M+H)^+$ 498.1917, found 498.1923.

*Diethyl 2-(4-(benzyloxy)phenyl)-2,3-dihydro-1H-naphtho[1,2-e][1,3]oxazine-1,3-dicarboxylate (**3ga**)*. Pale yellow oil (36.8 mg, 72% yield). ^{1}H NMR (400 MHz, $CDCl_3$) δ 7.79 (dd, J_1 = 8.3 Hz, J_2 = 5.8 Hz, 2H), 7.68 (d, J = 8.3 Hz, 1H), 7.50–7.45 (m, 1H), 7.40–7.29 (m, 7H), 7.26–7.19 (m, 2H), 6.85–6.78 (m, 2H), 6.29 (s, 1H), 5.26 (s, 1H), 4.98 (s, 2H), 4.41–4.29 (m, 2H), 4.24–4.11 (m, 2H), 1.36 (t, J = 7.1 Hz, 3H), 1.10 (t, J = 7.1 Hz, 3H); ^{13}C {^{1}H}NMR (100 MHz, $CDCl_3$) δ 171.2, 166.1, 156.5, 151.8, 140.3, 136.8, 131.2, 129.9, 129.5, 128.8, 128.5, 127.9, 127.4, 127.1, 126.3, 124.0, 121.6, 119.2, 115.2, 110.4, 83.1, 70.1, 63.7, 61.8, 14.2, 13.9; HRMS (ESI) calcd for $C_{31}H_{30}NO_6$ $(M+H)^+$ 512.2073, found 512.2079.

*Diethyl 2-(2,5-dimethoxyphenyl)-2,3-dihydro-1H-naphtho[1,2-e][1,3]oxazine-1,3-dicarboxylate (**3ha**)*. Pale yellow solid (38.6 mg, 83% yield), mp 116–117 °C. ^{1}H NMR (400 MHz, $CDCl_3$) δ 7.97 (d, J = 8.5 Hz, 1H), 7.83 (dd, J_1 = 8.4 Hz, J_2 = 4.8 Hz, 2H), 7.57–7.49 (m, 1H), 7.46–7.38 (m, 2H), 7.34 (d, J = 2.1 Hz, 1H), 6.65 (s, 1H), 6.54 (d, J = 2.7 Hz, 1H), 6.31 (dd, J_1 = 8.8 Hz, J_2 = 2.7 Hz, 1H), 5.36 (s, 1H), 4.40–4.31 (m, 3H), 4.19–4.15 (m, 1H), 3.98 (s, 3H), 3.79 (s, 3H), 1.38 (t, J = 7.1 Hz, 3H), 1.08 (t, J = 7.1 Hz, 3H); ^{13}C {^{1}H}NMR (100 MHz, $CDCl_3$) δ 158.2, 154.9, 151.3, 131.5, 129.8, 129.5, 129.1, 128.6, 126.7, 124.5, 123.8, 122.3, 119.2, 110.2, 103.3, 100.2, 83.2,

61.6, 61.5, 61.2, 56.0, 55.4, 14.1, 13.8; HRMS (ESI) calcd for $C_{26}H_{28}NO_7$ $(M+H)^+$ 466.1866, found 466.1872.

Diethyl 2-(4-methoxy-2-methylphenyl)-2,3-dihydro-1H-naphtho[1,2-e][1,3]oxazine-1,3-dicarboxylate ***(3ia)***. Pale yellow oil (34.6 mg, 77% yield). ^{1}H NMR (400 MHz, $CDCl_3$) δ 7.80 (d, J = 9.3 Hz, 2H), 7.67 (d, J = 8.4 Hz, 1H), 7.48–7.42 (m, 1H), 7.42–7.32 (m, 2H), 7.21 (d, J = 8.8 Hz, 1H), 6.75 (d, J = 2.9 Hz, 1H), 6.49 (dd, J_1 = 8.8 Hz, J_2 = 2.9 Hz, 1H), 6.32 (s, 1H), 4.97 (s, 1H), 4.37–4.34 (m, 2H), 4.14–4.02 (m, 2H), 3.71 (s, 3H), 2.49 (s, 3H), 1.36 (t, J = 7.1 Hz, 3H), 1.03 (t, J = 7.1 Hz, 3H); ^{13}C {^{1}H}NMR (100MHz, $CDCl_3$) δ 171.3, 165.9, 157.9, 151.6, 138.3, 131.4, 129.9, 129.5, 128.8, 127.4, 127.0, 123.9, 121.6, 119.3, 116.2, 110.9, 110.1, 83.4, 61.6, 61.5, 55.2, 18.7, 14.2, 13.7; HRMS (ESI) calcd for $C_{26}H_{28}NO_6$ $(M+H)^+$ 450.1917, found 450.1923.

Dimethyl 2-(4-methoxyphenyl)-2,3-dihydro-1H-naphtho[1,2-e][1,3]oxazine-1,3-dicarboxylate ***(3ja)***. White solid (32.2 mg, 79% yield), mp 115–116 °C. ^{1}H NMR (400 MHz, $CDCl_3$) δ 7.80 (dd, J_1 = 8.4 Hz, J_2 = 4.1 Hz, 2H), 7.64 (d, J = 8.3 Hz, 1H), 7.51–7.45 (m, 1H), 7.39 (t, J = 7.1 Hz, 1H), 7.33 (d, J = 8.9 Hz, 1H), 7.21 (d, J = 9.0 Hz, 2H), 6.74 (d, J = 9.0 Hz, 2H), 6.30 (s, 1H), 5.29 (s, 1H), 3.89 (s, 3H), 3.72 (s, 6H); ^{13}C {^{1}H}NMR (100 MHz, $CDCl_3$) δ 166.5, 157.4, 151.8, 139.9, 131.2, 130.1, 129.5, 128.9, 127.3, 126.1, 124.1, 121.5, 119.1, 114.3, 110.3, 83.2, 63.6, 55.3, 52.9, 52.7; HRMS (ESI) calcd for $C_{23}H_{22}NO_6$ $(M+H)^+$ 408.1447, found 408.1452.

Diisopropyl 2-(4-methoxyphenyl)-2,3-dihydro-1H-naphtho[1,2-e][1,3]oxazine-1,3-dicarboxylate ***(3ka)***. Pale yellow solid (38.5 mg, 83% yield), mp 122–123 °C. ^{1}H NMR (400 MHz, $CDCl_3$) δ 7.79 (dd, J_1 = 8.4 Hz, J_2 = 5.5 Hz, 2H), 7.66 (d, J = 8.4 Hz, 1H), 7.49–7.43 (m, 1H), 7.36 (dd, J_1 = 13.5Hz, J_2 = 8.1 Hz, 2H), 7.27–7.22 (m, 2H), 6.75 (d, J = 9.0 Hz, 2H), 6.22 (s, 1H), 5.23–5.19 (m, 2H), 5.08–4.95 (m, 1H), 3.72 (s, 3H), 1.34 (dd, J_1 = 6.2 Hz, J_2 = 3.2 Hz, 6H), 1.20 (d, J = 6.3 Hz, 3H), 1.01 (d, J = 6.2 Hz, 3H); ^{13}C {^{1}H}NMR (100 MHz, $CDCl_3$) δ 170.8, 165.6, 157.3, 151.9, 140.2, 131.3, 129.8 129.4, 128.8, 126.9, 126.5, 123.9, 121.7, 119.2, 114.0, 110.5, 83.1, 69.5, 69.3, 63.9, 55.3, 21.7, 21.6, 21.5, 21.2; HRMS (ESI) calcd for $C_{27}H_{30}NO_6$ $(M+H)^+$ 464.2073, found 464.2069.

Di-tert-butyl 2-(4-methoxyphenyl)-2,3-dihydro-1H-naphtho[1,2-e][1,3]oxazine-1,3-dicarboxylate ***(3la)***. Pale yellow oil (38.3 mg, 78% yield). ^{1}H NMR (400 MHz, $CDCl_3$) δ 7.77 (t, J = 8.7 Hz, 2H), 7.63 (d, J = 8.4 Hz, 1H), 7.48–7.44 (m, 1H), 7.38–7.31 (m, 2H), 7.30–7.26 (m, 2H), 6.14–6.04 (m, 1H), 5.09 (s, 1H), 3.73 (s, 3H), 1.56 (s, 9H), 1.30 (s, 9H); ^{13}C {^{1}H}NMR (100 MHz, $CDCl_3$) δ

170.6, 165.1, 157.1, 152.0, 140.5, 131.4, 129.7, 129.4, 128.7, 126.9, 126.4, 123.8, 121.7, 119.2, 113.9, 110.8, 82.9, 82.4, 82.2, 64.9, 55.4, 27.9, 27.6; HRMS (ESI) calcd for $C_{29}H_{34}NO_6$ $(M+H)^+$ 492.2386, found 492.2391.

*Dibenzyl 2-(4-methoxyphenyl)-2,3-dihydro-1H-naphtho[1,2-e][1,3]oxazine-1,3-dicarboxylate (**3ma**).* Pale yellow oil (44.8 mg, 80% yield). ^{1}H NMR (400 MHz, $CDCl_3$) δ 7.80 (dd, J_1 = 6.9 Hz, J_2 = 4.5 Hz, 2H), 7.63–7.56 (m, 1H), 7.39–7.36 (m, 4H), 7.36–7.26 (m, 7H), 7.21–7.15 (m, 4H), 6.67 (d, J = 9.0 Hz, 2H), 6.33 (s, 1H), 5.44–5.25 (m, 3H), 5.22 (d, J = 12.1 Hz, 1H), 5.11 (d, J = 12.1 Hz, 1H), 3.72 (s, 3H); ^{13}C {^{1}H}NMR (100 MHz, $CDCl_3$) δ 170.9, 165.9, 157.3, 151.8, 139.9, 135.3, 134.8, 131.1, 130.0, 129.4, 128.8, 128.6, 128.5, 128.4, 128.3, 128.2, 128.0, 127.1, 126.1, 124.0, 121.5, 119.1, 114.2, 110.1, 83.1, 67.3, 67.2, 63.8, 55.2; HRMS (ESI) calcd for $C_{35}H_{30}NO_6$ $(M+H)^+$ 560.2073, found 560.2069.

*Diethyl 9-bromo-2-(4-methoxyphenyl)-2,3-dihydro-1H-naphtho[1,2-e][1,3]oxazine-1,3-dicarboxylate (**3ab**).* Pale red oil (39.6 mg, 77% yield). ^{1}H NMR (400 MHz, $CDCl_3$) δ 7.92 (s, 1H), 7.73 (d, J = 9.0 Hz, 1H), 7.65 (d, J = 8.7 Hz, 1H), 7.49–7.41 (m, 1H), 7.33 (d, J = 9.0 Hz, 1H), 7.22 (d, J = 9.0 Hz, 2H), 6.76 (d, J = 4.0 Hz, 1H), 6.74 (d, J = 4.1 Hz, 1H), 6.35 (s, 1H), 5.19 (s, 1H), 4.47–4.42 (m, 1H), 4.33–4.28 (m, 1H), 4.26 – 4.11 (m, 2H), 3.72 (s, 3H), 1.40 (t, J = 7.1 Hz, 3H), 1.12 (t, J = 7.1 Hz, 3H); ^{13}C {^{1}H}NMR (100 MHz, $CDCl_3$) δ 171.1, 166.0, 157.5, 152.6, 139.8, 132.5, 130.3, 129.8, 129.4, 127.9, 127.4, 126.3, 124.4, 121.6, 119.6, 116.6, 114.3, 109.7, 83.2, 63.2, 62.0, 61.9, 55.4, 14.1, 13.9; HRMS (ESI) calcd for $C_{25}H_{25}BrNO_6$ $(M+H)^+$ 514.0865, found 514.0871, 516.0851 (isotopic mass).

*Diethyl 8-bromo-2-(4-methoxyphenyl)-2,3-dihydro-1H-naphtho[1,2-e][1,3]oxazine-1,3-dicarboxylate (**3ac**).* Pale yellow solid (37.6 mg, 73% yield), mp 140–141 °C. ^{1}H NMR (400 MHz, $CDCl_3$) δ 7.93 (d, J = 1.8 Hz, 1H), 7.68 (d, J = 9.0 Hz, 1H), 7.58–7.51(m, 2H), 7.34 (d, J = 9.0 Hz, 1H), 7.25–7.18 (m, 2H), 6.78–6.72 (m, 2H), 6.28 (s, 1H), 5.22 (s, 1H), 4.37–4.32 (m, 2H), 4.20–4.16 (m, 2H), 3.72 (s, 3H), 1.34 (t, J = 7.1 Hz, 3H), 1.11 (t, J = 7.1 Hz, 3H); ^{13}C {^{1}H}NMR (100 MHz, $CDCl_3$) δ 170.9, 165.9, 157.5, 152.1, 139.9, 130.7, 130.2, 129.8, 129.0, 126.3, 123.5, 120.3, 117.7, 116.6, 114.2, 110.7, 83.2, 63.5, 61.9, 61.8, 55.3, 14.1, 13.8; HRMS (ESI) calcd for $C_{25}H_{25}BrNO_6$ $(M+H)^+$ 514.0865, found 514.0870, 516.0850 (isotopic mass).

*Diethyl 8-cyano-2-(4-methoxyphenyl)-2,3-dihydro-1H-naphtho[1,2-e][1,3]oxazine-1,3-dicarboxylate (**3ad**).* White solid (37.8 mg, 82% yield), mp 135–136 °C. ^{1}H NMR (400 MHz,

$CDCl_3$) δ 8.15 (d, J = 1.4 Hz, 1H), 7.83 (d, J = 9.1 Hz, 1H), 7.76 (d, J = 8.8 Hz, 1H), 7.60 (dd, J_1 = 8.8 Hz, J_2 = 1.7 Hz, 1H), 7.44 (d, J = 9.0 Hz, 1H), 7.24–7.17 (m, 2H), 6.79–6.72 (m, 2H), 6.30 (s, 1H), 5.23 (s, 1H), 4.44–4.30 (m, 2H), 4.25–4.11 (m, 2H), 3.72 (s, 3H), 1.35 (t, J = 7.1 Hz, 3H), 1.11 (t, J = 7.1 Hz, 3H); ^{13}C {^1H}NMR (100 MHz, $CDCl_3$) δ 170.7, 165.5, 157.6, 154.3, 139.6, 134.5, 133.1, 130.4, 128.5, 127.8, 126.2, 122.9, 121.2, 119.0, 114.3, 110.8, 107.4, 83.4, 63.4, 62.1, 62.0, 55.3, 14.1, 13.8; HRMS (ESI) calcd for $C_{26}H_{25}N_2O_6$ $(M+H)^+$ 461.1713, found 461.1718.

*1,3-Bis(ethoxycarbonyl)-2-(4-methoxyphenyl)-2,3-dihydro-1H-naphtho[1,2-e][1,3]oxazine-8-carb-oxylic acid (**3ae**).* Pale yellow solid (35.0 mg, 73% yield), mp 152–153 °C. ^1H NMR (400 MHz, Acetone-*d*6) δ 8.61 (d, J = 1.6 Hz, 1H), 8.10–8.06 (m, 2H), 7.85 (d, J = 9.1 Hz, 1H), 7.37 (d, J = 9.0 Hz, 1H), 7.23–7.20 (m, 2H), 6.82–6.79 (m, 2H), 6.24 (s, 1H), 5.41 (s, 1H), 4.35–4.30 (m, 2H), 4.15–4.12 (m, 2H), 3.71 (s, 3H), 1.32 (t, J = 7.1 Hz, 3H), 1.08 (t, J = 7.1 Hz, 3H); ^{13}C {^1H}NMR (100 MHz, $CDCl_3$) δ 171.8, 170.9, 165.8, 157.5, 154.1, 139.8, 134.3, 132.7, 131.5, 128.6, 126.8, 126.3, 124.7, 122.1, 120.3, 114.3, 110.7, 83.3, 63.6, 62.0, 61.9, 55.4, 14.2, 13.9; HRMS (ESI) calcd for $C_{26}H_{26}NO_8$ $(M+H)^+$ 480.1658, found 480.1663.

*1,3-Diethyl 8-methyl 2-(4-methoxyphenyl)-2,3-dihydro-1H-naphtho[1,2-e][1,3]oxazine-1,3,8-tricarboxylate (**3af**).* Pale yellow solid (36.5 mg, 74% yield), mp 158–159 °C. ^1H NMR (400 MHz, Acetone-*d*6) δ 8.58 (d, J = 1.4 Hz, 1H), 8.11–8.03 (m, 2H), 7.85 (d, J = 9.0 Hz, 1H), 7.38 (d, J = 9.0 Hz, 1H), 7.21 (d, J = 9.0 Hz, 2H), 6.82–6.79 (m, 2H), 6.24 (s, 1H), 5.41 (s, 1H), 4.37–4.28 (m, 2H), 4.16–4.10 (m, 2H), 3.92 (s, 3H), 3.71 (s, 3H), 1.32 (t, J = 7.1 Hz, 3H), 1.08 (t, J = 7.1 Hz, 3H); ^{13}C {^1H}NMR (100 MHz, $CDCl_3$) δ 170.9, 166.9, 165.7, 157.5, 153.8, 139.8, 133.7, 131.6, 131.3, 128.6, 126.6, 126.2, 125.5, 121.9, 120.1, 114.2, 110.6, 83.3, 63.5, 61.9, 61.8, 55.3, 52.1, 14.1, 13.8; HRMS (ESI) calcd for $C_{27}H_{28}NO_8$ $(M+H)^+$ 494.1815, found 494.1819.

*Diethyl 9-hydroxyl-2-(4-methoxyphenyl)-2,3-dihydro-1H-naphtho[1,2-e][1,3]oxazine-1,3-di-carboxylate (**3ag**).* Pale yellow solid (35.7 mg, 79% yield), mp 141–142 °C. ^1H NMR (400 MHz, $CDCl_3$) δ 7.66 (dd, J_1 = 8.8 Hz, J_2 = 6.7 Hz, 2H), 7.24–7.18 (m, 2H), 7.14 (d, J = 9.0 Hz, 1H), 7.02 (d, J = 2.2 Hz, 1H), 6.95 (dd, J_1 = 8.8 Hz, J_2 = 2.3 Hz, 1H), 6.75–6.67 (m, 2H), 6.26 (s, 1H), 5.12 (s, 1H), 4.42–4.32 (m, 1H), 4.32–4.24 (m, 1H), 4.24–4.12 (m, 2H), 3.70 (s, 3H), 1.32 (t, J = 7.1 Hz, 3H), 1.11 (t, J = 7.1 Hz, 3H); ^{13}C {^1H}NMR (100 MHz, $CDCl_3$) δ 171.4, 166.3, 157.4, 154.9, 152.4, 140.1, 132.7, 130.7, 129.7, 126.3, 124.6, 116.5, 115.5, 114.2, 109.0, 104.6, 83.2, 63.9, 61.9, 61.8, 55.3, 14.0, 13.9; HRMS (ESI) calcd for $C_{25}H_{26}NO_7$ $(M+H)^+$ 452.1709, found

452.1713.

*Diethyl 9-methoxy-2-(4-methoxyphenyl)-2,3-dihydro-1H-naphtho[1,2-e][1,3]oxazine-1,3-dicarboxylate (**3ah**).* Pale yellow oil (37.5 mg, 81% yield). ^{1}H NMR (400 MHz, Acetone-*d*6) δ 7.79 (t, J = 8.8 Hz, 2H), 7.21–7.18 (m, 2H), 7.11–7.05 (m, 3H), 6.80 (d, J = 9.0 Hz, 2H), 6.24 (s, 1H), 5.28 (s, 1H), 4.35–4.30 (m, 2H), 4.14–4.09 (m, 2H), 3.88 (s, 3H), 3.71 (s, 3H), 1.33 (t, J = 7.1 Hz, 3H), 1.08 (t, J = 7.1 Hz, 3H); ^{13}C {^{1}H}NMR (100 MHz, $CDCl_3$) δ 171.3, 166.2, 158.8, 157.5, 152.5, 140.1, 132.5, 130.3, 129.6, 129.4, 126.5, 124.7, 116.6, 116.5, 116.1, 114.2, 109.5, 101.1, 83.2, 63.8, 61.8, 55.4, 55.2, 14.2, 13.9; HRMS (ESI) calcd for $C_{26}H_{28}NO_7$ $(M+H)^+$ 466.1866, found 466.1872.

*Diethyl 9-ethoxy-2-(4-methoxyphenyl)-2,3-dihydro-1H-naphtho[1,2-e][1,3]oxazine-1,3-dicarboxylate(**3ai**).* White solid (40.8 mg, 85% yield), mp 111–112 °C. ^{1}H NMR (400 MHz, $CDCl_3$) δ 7.69 (dd, J_1 = 8.9 Hz, J_2 = 4.7 Hz, 2H), 7.23 (d, J = 8.9 Hz, 2H), 7.18 (d, J = 8.9 Hz, 1H), 7.02 (dd, J_1 = 8.9 Hz, J_2 = 2.2 Hz, 1H), 6.97 (d, J = 2.0 Hz, 1H), 6.79–6.67 (m, 2H), 6.30 (s, 1H), 5.15 (s, 1H), 4.39–4.29 (m, 2H), 4.25–4.14 (m, 2H), 4.13–4.01 (m, 2H), 3.73 (s, 3H), 1.46 (t, J = 7.0 Hz, 3H), 1.34 (t, J = 7.1 Hz, 3H), 1.12 (t, J = 7.1 Hz, 3H); ^{13}C {^{1}H}NMR (100 MHz, $CDCl_3$) δ 171.3, 166.2, 158.1, 157.4, 152.4, 140.1, 132.5, 130.3, 129.6, 126.5, 124.6, 116.5, 116.4, 114.2, 109.4, 101.7, 83.2, 63.9, 63.4, 61.8, 61.7, 55.4, 14.8, 14.2, 13.9; HRMS (ESI) calcd for $C_{27}H_{30}NO_7$ $(M+H)^+$ 480.2022, found 480.2026.

*Diethyl 8-(hydroxymethyl)-2-(4-methoxyphenyl)-2,3-dihydro-1H-naphtho[1,2-e][1,3]oxazine-1,3-dicarboxylate (**3aj**).* Pale yellow oil (30.3 mg, 65% yield). ^{1}H NMR (400 MHz, $CDCl_3$) δ 7.79–7.74 (m, 2H), 7.68 (d, J = 8.7 Hz, 1H), 7.48 (dd, J_1 = 8.7 Hz, J_2 = 1.7 Hz, 1H), 7.33 (d, J = 9.0 Hz, 1H), 7.25–7.19 (m, 2H), 6.76–6.71 (m, 2H), 6.28 (s, 1H), 5.24 (s, 1H), 4.81 (s, 2H), 4.40–4.28 (m, 2H), 4.22–4.13 (m, 2H), 3.72 (s, 3H), 1.35 (t, J = 7.1 Hz, 3H), 1.11 (t, J = 7.1 Hz, 3H); ^{13}C {^{1}H}NMR (100 MHz, $CDCl_3$) δ 171.2, 166.1, 157.4, 151.9, 140.0, 136.5, 130.7, 129.9, 129.4, 126.5, 126.4, 126.3, 122.1, 119.5, 114.2, 110.5, 83.2, 65.1, 63.7, 61.9, 61.8, 55.3, 14.1, 13.9; HRMS (ESI) calcd for $C_{26}H_{28}NO_7$ $(M+H)^+$ 466.1866, found 466.1872.

*Ethyl 2-(4-hydroxynaphthalen-1-yl)-2-((4-methoxyphenyl)amino)acetate(**4ak**).* [18e] Pale red oil (23.9 mg, 68% yield). ^{1}H NMR (400 MHz, $CDCl_3$) δ 8.31–8.23 (m, 1H), 7.83–7.77 (m, 1H), 7.49 (m, 2H), 7.43 (d, J = 8.5 Hz, 1H), 7.37 (d, J = 8.5 Hz, 1H), 6.79 (m, 2H), 6.75 (m, 2H), 5.08 (s, 1H), 4.33–4.25 (m, 1H), 4.21–4.13 (m, 1H), 3.72 (s, 3H), 1.22 (t, J = 7.1 Hz, 3H); ^{13}C {^{1}H}NMR

(100 MHz, $CDCl_3$) δ 171.2, 154.6, 153.0, 138.8, 134.1, 127.2, 126.8, 126.6, 125.4, 125.2, 122.4, 119.4, 117.8, 114.7, 113.2, 63.4, 62.4, 55.5, 13.9. The obtained spectra match those previously reported.

*Ethyl 2-(6-hydroxybenzo[d][1,3]dioxol-5-yl)-2-((4-methoxyphenyl)amino)acetate(**4al**).*[18e] White solid (20.0 mg, 58% yield), mp 116–117 °C. ^{1}H NMR (400 MHz, $CDCl_3$) δ 9.12 (s, 1H), 6.80–6.72 (m, 4H), 6.70 (s, 1H), 6.42 (s, 1H), 5.92 (s, 2H), 4.85 (s, 1H), 4.72 (s, 1H), 4.34–4.24 (m, 1H), 4.23–4.13 (m, 1H), 3.74 (s, 3H), 1.25 (t, J = 7.1 Hz, 3H); ^{13}C {^{1}H}NMR (100 MHz, $CDCl_3$) δ 171.2, 154.4, 151.9, 148.3, 141.0, 138.8, 117.6, 114.7, 112.3, 108.2, 101.1, 99.5, 62.4, 55.5, 14.0. The obtained spectra match those previously reported.

*Ethyl 2-(2,6-dihydroxyphenyl)-2-((4-methoxyphenyl)amino)acetate(**4am**).*[18e] White solid (14.3 mg, 45% yield), mp 68–69 °C. ^{1}H NMR (400 MHz, $CDCl_3$) δ 7.05 (d, J = 8.3 Hz, 1H), 6.78–6.73 (m, 4H), 6.39 (dd, J = 8.3, 2.5 Hz, 1H), 6.35 (d, J = 2.4 Hz, 1H), 4.94 (s, 1H), 4.30–4.24 (m, 1H), 4.22–4.15 (m, 1H), 3.73 (s, 3H), 1.22 (t, J = 7.1 Hz, 3H); ^{13}C {^{1}H}NMR (100 MHz, $CDCl_3$) δ 171.7, 157.5, 157.2, 154.4, 138.9, 130.2, 117.8, 114.7, 113.3, 107.7, 104.3, 62.3, 62.1, 55.5, 14.0. The obtained spectra match those previously reported.

Procedure for the Synthesis of Arylglycine 6.

3aa (65 mg, 0.15 mmol) was dissolved in anhydrous ethanol (1.0 mL), then NaOH (42 mg, 1.05 mmol) was added to the solution. The mixture was heated to 70 °C and stirred at this temperature for 1 h. The mixture was poured into 3 M HCl and filtered out the salt. The solvent was removed by *vacuo*. The residue was suspended in CH_2Cl_2, then filtered (washed with CH_2Cl_2), arylglycine **6** was obtained as a pale yellow solid (21.2 mg, 65%), mp 134−136 °C. ^{1}H NMR (400 MHz, CD_3OD) δ 7.80 (t, J = 9.0 Hz, 2H), 7.73 (d, J = 8.0 Hz, 1H), 7.40 (t, J = 7.6 Hz, 1H), 7.29–7.21 (m, 3H), 7.18 (d, J = 8.9 Hz, 1H), 6.74 (d, J = 9.0 Hz, 2H), 6.25 (s, 1H), 3.63 (s, 3H); ^{13}C {^{1}H}NMR (101 MHz, CD_3OD) δ 171.0, 161.6, 133.6, 129.93, 129.88, 128.7, 127.4, 126.0, 125.2, 124.3, 122.0, 117.9, 116.3, 115.5, 108.9, 61.9, 55.9. HRMS (ESI) calcd for $C_{19}H_{17}NO_6$ $(M+H)^+$ 324.1230, found 324.1226.

Procedure for the Esterification of 3ae with Podophyllotoxin 7.

Podophyllotoxin **7** (62 mg, 0.15 mmol) was dissolved in anhydrous CH_2Cl_2 (2 mL), then **3ae** (47.9 mg, 0.1 mmol), DCC (61.8 mg, 0.3 mmol), and DMAP (1.2 mg, 10 mol%) were added respectively, the solution was stirred at room temperature. After the reaction was completed as

monitored by TLC, 3 M HCl was added. The mixture was extracted with CH_2Cl_2 (5 mL × 3). The organic layer was combined, washed with water and brine respectively, dried over anhydrous Na_2SO_4, and concentrated in *vacuo*. The crude product was purified by column chromatography (petroleum ether/ethyl acetate = 1:1) to give ester **8** as a white solid (54.7 mg, 72%), mp 150–152 °C. ^{1}H NMR ($CDCl_3$, 400 MHz) δ 8.52 (s, 1H), 8.01 (ddd, J = 8.9, 3.4, 1.8 Hz, 1H), 7.86 (d, J = 8.9 Hz, 1H), 7.73 (dd, J = 8.8, 6.7 Hz, 1H), 7.41 (d, J = 9.0 Hz, 1H), 7.21 (dd, J = 9.0, 0.9 Hz, 2H), 6.89 (s, 1H), 6.74 (d, J = 8.9 Hz, 2H), 6.59 (s, 1H), 6.46 (d, J = 1.0 Hz, 2H), 6.29 (d, J = 6.4 Hz, 1H), 6.16 (d, J = 6.7 Hz, 1H), 6.03–5.95 (m, 2H), 5.25 (s, 1H), 4.66 (d, J = 3.1 Hz, 1H), 4.50–4.43 (m, 1H), 4.39–4.28 (m, 3H), 4.23–4.11 (m, 2H), 3.79 (s, 9H), 3.71 (s, 3H), 3.06–2.96 (m, 2H), 1.34 (td, J = 7.1, 4.9 Hz, 3H), 1.10 (t, J = 7.1 Hz, 3H); ^{13}C {^{1}H}NMR (101 MHz, $CDCl_3$) δ 173.7, 170.8, 166.7, 165.6, 157.5, 154.2, 152.6, 148.2, 147.7, 139.7, 137.0, 134.8, 134.1, 132.4, 132.0, 131.3, 128.5, 128.3, 126.3, 126.2, 124.5, 122.3, 120.5, 114.2, 110.7, 109.7, 108.0, 107.1, 101.6, 83.3, 74.2, 71.5, 63.5, 62.0, 61.9, 60.7, 56.1, 55.3, 45.6, 43.7, 38.8, 14.2, 13.8; HRMS (ESI) calcd for $C_{48}H_{45}NO_{15}$ $(M+H)^+$ 876.2867, found 876.2861.

ASSOCIATED CONTENT

Supporting Information

The Supporting Information is available free of charge via the Internet at http://pubs.acs.org.

Optimization of Reaction Conditions; X-Ray Single Crystal Diffraction Data for **3aa**; Copies of ^{1}H and ^{13}C NMR spectra of synthetic compounds.

AUTHOR INFORMATION

Corresponding Author

*E-mail: zhangyuan@lzu.edu.cn

*E-mail: liying@lzu.edu.cn

Notes

The authors declare no competing financial interest.

ACKNOWLEDGMENT

We gratefully acknowledge the National Natural Science Foundation of China (Nos. 21572092 and 21772079) and Natural Science Foundation of Gansu Province (18JR4RA003) for financial

support. We thank professor Qiang Liu (Lanzhou University) for helpful discussion. We also thank Mr. Shutao Wang (Lanzhou University) for computational studies.

REFERENCES

(1) Benameur, L.; Bouaziz, Z.; Nebois, P.; Bartoli, M.-H.; Boitard, M.; Fillion, H.Synthesis of Furnaphth[1,3]oxazine and Furo[1, 3]oxazinoquinoline Derivatives as Precursors for an *o*-Quinonemethide Structure and Potential Antitumor Agents. *Chem. Pharm. Bull.* **1996**, *44*, 605−608.

(2) (a) Waissera, K.; Gregora, J.; Kubicováa, L.; Klimesováa, V.; Kunesab, J.; Kaustovác, J. New Groups of Antimycobacterial Agents: 6-Chloro-3-phenyl-4-thioxo-2H-1,3-benzoxazine-2(3H)-ones and 6-Chloro-3-phenyl-2H-1,3-benzoxazine-2,4(3H)-dithiones. *Eur. J. Med. Chem.* **2000**, *35*, 733−741. (b) Mathew, B. P.; Kumar, A.; Sharma, S.; Shukla, P. K.; Nath, M. An Eco-Friendly Synthesis and Antimicrobial Activities of Dihydro-2H-benzo- and Naphtho-1,3-oxazine Derivatives. *Eur. J. Med. Chem.* **2010**, *45*, 1502−1507.

(3) Cocuzza, A. J.; Chidester, D. R.; Cordova, B. C.; Jeffrey, S.; Parsons, R. L.; Bacheler, L. T.; Viitanen, S. E.; Trainor, G.L.; Ko, S. S. Synthesis and Evaluation of Efavirenz (Sustiva™) Analogues as HIV-1 Reverse Transcriptase Inhibitors: Replacement of the Cyclopropylacetylene Side Chain. *Bioorg. Med. Chem. Lett.* **2001**, *11*, 1177–1179.

(4) (a) Joyce, J. N.; Presgraves, S.; Renish, L.; Borwege, S.; Osredkar, T.; Hagner, D.; Replogle, M.; PazSoldan, M.; Millanb, M. J. Neuroprotective Effects of the Novel D3/D2 Receptor Agonist and Antiparkinson Agent, S32504, in vitro against 1-Methyl-4-phenylpyridinium (MPP+) and in vivo against 1-Methyl-4-phenyl-1,2,3,6-tetrahydropyridine (MPTP): A Comparison to Ropinirole. *Experimental Neurology* **2003**, *184*, 393–407. (b) Augelli−Szafran, C. E.; Jaen, J. C.; Moreland, D. W.; Nelson, C. B.; Penvose-Yi, J. R.; Schwarz, R. D. Identification and Characterization of M4 Selective Muscarinic Antagonists. *Bioorg. Med. Chem. Lett.* **1998**, *8*, 1991−1996. (c) Bohme, T. M.; Augelli−Szafran, C. E.; Hallak, H.; Pugsley, T.; Serpa, K.; Schwarz, R. D. Synthesis and Pharmacology of Benzoxazines as Highly Selective Antagonists at M4 Muscarinic Receptors. *J. Med. Chem.* **2002**, *45*, 3094−3102.

(5) (a) Yamazaki, N.; Ito, T.; Kibayashi, C. Asymmetric Synthesis of (−)-Indolizidines 167B and 209D Based on Stereocontrolled Allylation of a Chiral Tricyclic N-Acyl-N,O-acetal. *Org. Lett.* **2000**, *2*, 465−467. (b) Cheng, G. L.; Wang, X. Y.; Su, D. Y.; Liu, H.; Liu, F.; Hu, Y. F. Preparation of Enantiopure Substituted Piperidines Containing 2-Alkene or 2-Alkyne Chains: Application to Total Syntheses of Natural Quinolizidine-Alkaloids. *J. Org. Chem.* **2010**, *75,* 1911−1916.

(6) (a) Jin, L.; Agag, T.; Yagci, Y.; Ishida, H. Methacryloyl-Functional Benzoxazine: Photopolymerization and Thermally Activated Polymerization. *Macromolecules* **2011**, *44*, 767−772. (b) Arza, R.; Maurer, F. H. J.; Ishida, H. Primary Amine-Functional Benzoxazine Monomers and Their Use for Amide-Containing Monomeric Benzoxazines. *Macromolecules* **2010**, *43*, 2748−2758.

(7) For recent examples, see: (a) Mulzer, M.; Coates, G. W. A Catalytic Route to Ampakines and Their Derivatives. *Org. Lett.* **2011**, *13*, 1426−1428. (b) Vellalath, S.; Coric, I.; List, B. N-Phosphinyl Phosphoramide-A Chiral Brønsted Acid Motif for the Direct Asymmetric N,O-Acetalization of Aldehydes. *Angew. Chem. Int. Ed.* **2010**, *49*, 9749−9752. (c) Jurberg, I. D.; Peng, B.; Wostefeld, E.; Wasserloos, M.; Maulide, N. Intramolecular Redox-Triggered C-H Functionalization. *Angew. Chem. Int. Ed.* **2012**, *51*, 1950−1953. (d) Richers, M. T.; Breugst, M.; Platonova, A. Y.; Ullrich, A.; Dieckmann, A.; Houk, K. N.; Seidel, D. Redox-Neutral α-Oxygenation of Amines: Reaction Development and Elucidation of the Mechanism. *J. Am. Chem. Soc.* **2014**, *136*, 6123−6135. (e) Gonzalez−Rodriguez, C.; Suarez, J. R.; Varela, J. A.; Saa, C. Nucleophilic Addition of Amines to Ruthenium Carbenes:ortho-(Alkynyloxy)benzyl-amine Cyclizations towards 1,3- Benzoxazines. *Angew. Chem. Int. Ed.* **2015**, *54*, 2724–2728. (f) Gupta, K. S. V.; Ramana, D. V.; Vinayak, B.; Sridhar, B.; Chandrasekharam, M. Copper-Catalyzed Regio and Diastereoselective Three Component C–N, C–C and C–O Bond Forming Reaction: Oxidative sp^3 C–H Functionalization. *New J. Chem.* **2016**, *40*, 6389−6395. (g) Chen, X. W.; Hao, W. Y.; Liu, Y. Y. Copper-Catalyzed Tandem Aryl–Halogen Hydroxylation and CH_2Cl_2-based N,O-Acetalization toward the Synthesis of 2,3-Dihydrobenzoxazinones. *Org. Biomol. Chem.* **2017**, *15*, 3423–3426. (h) Chen, E.; Shao, J.; Tang, P.; Shu, K.; Chen, W.; Yu, Y. Catalyst-Free Three-component Sequencing for Efficient Assembly of [1,3] Oxazine N-Fused Imidazole-2-thiones. *Green Chem.* **2018**, *20*, 3696–3699.

(8) (a) Li, C. -J. Cross-Dehydrogenative Coupling (CDC): Exploring C−C Bond Formations beyond Functional Group Transformations. *Acc. Chem. Res.* **2009**, *42*, 335–344. (b) Girard, S. A.; Knauber, T.; Li, C. -J. The Cross-Dehydrogenative Coupling of C_{sp3}-H Bonds: A Versatile Strategy for C-C Bond Formations. *Angew. Chem. Int. Ed.* **2014**, *53*, 74–100. (c) Yeung, C. S.; Dong, V. M. Catalytic Dehydrogenative Cross-Coupling: Forming C-C Bonds by Oxidizing Two Carbon−Hydrogen Bonds. *Chem. Rev.* **2011**, *111*, 1215–1292. (d) Liu, C.; Zhang, H.; Shi, W.; Lei, A. Bond Formations between Two Nucleophiles: Transition Metal Catalyzed Oxidative Cross-Coupling Reactions. *Chem. Rev.* **2011**, *111*, 1780–1824. (e) Zhang, C.; Tang, C.; Jiao, N. Recent Advances in Copper-Catalyzed Dehydrogenative Functionalization via A Single Electron Transfer (SET) Process. *Chem. Soc. Rev.* **2012**, *41*, 3464–3484. (f) Qin, Y.; Zhu, L.; Luo, S. Organocatalysis in Inert C–H Bond Functionalization. *Chem. Rev.* **2017**, *117*, 9433–9520.

(9) For selected recent examples, see: (a) Neel, A. J.; Hehn, J. P.; Tripet, P. F.; Toste, F. D. Asymmetric Cross-Dehydrogenative Coupling Enabled by the Design and Application of Chiral Triazole-Containing Phosphoric Acids. *J. Am. Chem. Soc.* **2013**, *135*, 14044–14047. (b) Xie, Z.; Liu, L.; Chen, W.; Zheng, H.; Xu, Q.; Yuan, H.; Lou, H. Practical Metal-Free C(sp^3)-H Functionalization: Construction of Structurally Diverse α-Substituted N-Benzyl and N-Allyl Carbamates. *Angew. Chem. Int. Ed.* **2014**, *53*, 3904–3908. (c) Liu, X.; Meng, Z.; Li, C.; Lou, H.; Liu, L. Organocatalytic Enantioselective Oxidative C-H Alkenylation and Arylation of N-Carbamoyl Tetrahydropyridines and Tetrahydro-β-carbolines. *Angew. Chem. Int. Ed.* **2015**, *54*, 6012–6015. (d) Sun, S.; Li, C.; Floreancig, P. E.; Lou, H.; Liu, L. Highly Enantioselective Catalytic Cross-Dehydrogenative Coupling of N-Carbamoyl Tetrahydroisoquinolines and Terminal Alkynes. *Org. Lett.* **2015**, *17*, 1684–1687. (e) Wang, G.; Mao, Y.; Liu, L. Diastereoselectively Complementary C–H Functionalization Enables Access to Structurally and Stereochemically Diverse 2,6-Substituted Piperidines. *Org. Lett.* **2016**, *18*, 6476–6479. (f) Long, H.; Wang, G.; Lu, R.; Xu, M.; Zhang, K.; Qi, S.; He, Y.; Bu, Y.; Liu, L. Regio- and Diastereoselective Cross-Dehydrogenative Coupling of Tetrahydropyridines with 1,3-Dicarbonyl Compounds. *Org. Lett.* **2017**, *19*, 2146–2149. (g) Wu, Y.; Yi, H.; Lei, A. W. Electrochemical Acceptorless Dehydrogenation of N-Heterocycles Utilizing TEMPO as Organo-Electrocatalyst. *ACS Catal*. **2018**, *8*, 1192−1196. (h) Deb, M. L.; Pegu, C. D.; Borpatra, P. J.; Saikia, P. J.; Baruah, P. K., Catalyst-Free Multi-Component Cascade C–H-Functionalization in Water Using Molecular Oxygen: An Approach to 1,3-Oxazines. *Green Chem*. **2017**, *19*, 4036−4042. (i) Deb, M. L.; Borpatra, P. J.; Baruah, P. K., A One-Pot Catalyst/External Oxidant/Solvent-Free Cascade Approach to Pyrimidines via A 1,5-Hydride Transfer. *Green Chem.* **2019**, *21*, 69−74. (j) Huang, T.; Liu, X.; Lang, J.; Xu, J.; Lin, L.; Feng, X. Asymmetric Aerobic Oxidative Cross-Coupling of Tetrahydroisoquinolines with Alkynes. *ACS Cat.* **2017**, *7*, 5654−5660. (k) Liu, X.; Sun, S.; Meng, Z.; Lou, H.; Liu, L., Organocatalytic Asymmetric C–H Vinylation and Arylation of N-Acyl Tetrahydroisoquinolines. *Org. Lett.* **2015,** *17*, 2396−2399. (l) Xie, Z.; Zan, X.; Sun, S.; Pan, X.; Liu, L., Organocatalytic Enantioselective Cross-Dehydrogenative Coupling of N-Carbamoyl Cyclic Amines with Aldehydes. *Org. Lett.* **2016,** *18*, 3944−3947.

(10) (a) Xuan, J.; Feng, Z. J.; Duan, S. W.; Xiao, W. J. Room Temperature Synthesis of Isoquino[2,1-a][3,1]oxazine and Isoquino[2,1-a]pyrimidine Derivatives via Visible Light Photoredox Catalysis. *RSC Adv.* **2012**, *2*, 4065–4068. (b) Deb, M. L.; Dey, S. S.; Bento, I.; Barros, M. T.; Maycock, C. D. Copper-Catalyzed Regioselective Intramolecular Oxidative α-Functionalization of Tertiary Amines: An Efficient Synthesis of Dihydro-1,3-Oxazines. *Angew. Chem. Int. Ed.* **2013**, *52*, 9791–9795. (c) Mahato, S.; Haldar, S.; Jana, C. K. Diastereoselective α-C–H Functionalization of Aliphatic N-Heterocycles: An Efficient Route to Ring Fused

Oxazines. *Chem. Commun.* **2014**, *50*, 332–334. (d) Modak, A.; Dutta, U.; Kancherla, R.; Maity, S.; Bhadra, M.; Mobin, S. M.; Maiti, D. Predictably Selective (sp^3)C–O Bond Formation through Copper Catalyzed Dehydrogenative Coupling: Facile Synthesis of Dihydro-oxazinone Derivatives. *Org. Lett.* **2014**, *16*, 2602−2605. (e) Deb, M. L.; Pegu, C. D.; Borpatra, P. J.; Baruah, P. K. Metal-Free Intramolecular α-sp^3 C–H Oxygenation of tert-Amine: An Efficient Approach to 1,3-Oxazines. *Tetrahedron Lett.* **2016**, *57*, 5479–5483. (f) Borpatra, P. J.; Deb, M. L.; Baruah, P. K. Visible Light-Promoted Metal-Free Intramolecular Cross Dehydrogenative Coupling Approach to 1,3-Oxazines. *Tetrahedron Lett.* **2017**, *58*, 4006–4010. (g) Borpatra, P. J.; Deb, M. L.; Baruah, P. K. Copper-Catalyzed Tandem Multi-Component Approach to 1,3-Oxazines at Room Temperature by Cross-Dehydrogenative Coupling Using Methanol as C1 Feedstock. *Synlett* **2018**, *29*, 1171–1175. (h) Mathis, C. L.; Gist, B. M.; Frederickson, C. K.; Midkiff, K. M.; Marvin, C. C. Visible Light Photooxidative Cyclization of Amino Alcohols to 1,3-Oxazines. *Tetrahedron Lett.* **2013**, *54*, 2101–2104. (i) Rong, H. J.; Yao, J. J.; Li, J. K.; Qu, J. Molecular Iodine-Mediated α-C–H Oxidation of Pyrrolidines to N,O-Acetals: Synthesis of (±)-Preussin by Late-Stage 2,5-Difunctionalizations of Pyrrolidine. *J. Org. Chem.* **2017**, *82*, 5557−5565. (j) Martina, K.; Rotolo, L.; Porcheddu, A.; Delogu, F.; Bysouth, S. R.; Cravotto, G.; Colacino, E. High Throughput Mechanochemistry: Application to Parallel Synthesis of Benzoxazines. *Chem. Commun.* **2018**, *54*, 551–554. (k) Butler, J. D.; Solano, D. A.; Robins, L. I.; Haddadin, M. J.; Kurth, M. J. A Facile Synthesis of New 5H-Indazolo[3,2-b]benzo[d]-1,3-oxazines via One-Pot Intramolecular Bis-heterocyclizations. *J. Org. Chem.* **2008**, *73*, 234–240.

(11) Zhang, G. Y.; Xiang, Y.; Guan, Z.; He, Y. H. Enzyme and Photoredox Sequential Catalysis for the Synthesis of 1,3-Oxazine Derivatives in One Pot. *Catal. Sci. Techno.* **2017**, *7*, 1937–1942.

(12) Zhao, L.; Li, C. -J. Functionalizing Glycine Derivatives by Direct C-C Bond Formation. *Angew. Chem. Int. Ed.* **2008**, *47*, 7075–7078.

(13) (a) Zhao, L.; Baslé, O.; Li, C. -J. Site-Specific C–H Functionalization of Free-(NH) Peptides and Glycine Derivatives via Direct C–H Bond Functionalization. *Proc. Natl. Acad. Sci. USA* **2009**, *106*, 4106–4111. (b) Xie, J.; Huang, Z. Z. Cross-Dehydrogenative Coupling Reactions by Transition-Metal and Aminocatalysis for the Synthesis of Amino Acid Derivatives. *Angew. Chem. Int. Ed.* **2010**, *49*, 10181–10185. (c) Li, K.; Tan, G.; Huang, J.; Song, F.; You, J. Iron-Catalyzed Oxidative C-H/C-H Cross-Coupling: An Efficient Route to α-Quaternary α-Amino Acid Derivatives. *Angew. Chem. Int. Ed.* **2013**, *52*, 12942–12945. (d) Huo, C.; Yuan, Y.; Wu, M.; Jia, X.; Wang, X.; Chen, F.; Tang, J. Auto-Oxidative Coupling of Glycine Derivatives. *Angew. Chem. Int. Ed.* **2014**, *53*, 13544–13547. (e) Huo, C.; Wang, C.; Wu, M.; Jia, X.; Xie, H.; Yuan, Y. Copper(I) Chloride-Catalyzed Aerobic Oxidative

Arylation of Glycine Ester and Amide Derivatives. *Adv. Synth. Catal*. **2014**, *356*, 411–415. (f) Zhu, Z.-Q.; Bai, P.; Huang, Z.-Z. Dehydrogenative Cross-Coupling Reaction by Cooperative Transition-Metal and Brønsted Acid Catalysis for the Synthesis of *β*-Quinolinyl *α*-Amino Acid Esters. *Org. Lett.* **2014**, *16*, 4881–4883. (g) Salman, M.; Zhu, Z. Q.; Huang, Z. Z. Dehydrogenative Cross-Coupling Reaction between N-Aryl α-Amino Acid Esters and Phenols or Phenol Derivative for Synthesis of α-Aryl α-Amino Acid Esters. *Org. Lett.* **2016**, *18*, 1526–1529. (h) Xie, Z.; Liu, X.; Liu, L. Copper-Catalyzed Aerobic Enantioselective Cross-Dehydrogenative Coupling of N-Aryl Glycine Esters with Terminal Alkynes. *Org. Lett.* **2016**, *18*, 2982–2985. (i) Jia, X.; Liu, X.; Shao, Y.; Yuan, Y.; Zhu, Y.; Hou, W.; Zhang, X. Oxidative Phosphorylation of N-Aryl Glycine Amides via sp^3 C−H Functionalization. *Adv. Synth. Catal.* **2017**, *359*, 4399–4404.

(14) (a) Richter, H.; Mancheño, O. G. TEMPO Oxoammonium Salt-Mediated Dehydrogenative Povarov/Oxidation Tandem Reaction of N-Alkyl Anilines. *Org. Lett.* **2011**, *13*, 6066–6069. (b) Jia, X.; Peng, F.; Qing, C.; Huo, C.; Wang, X. Catalytic Radical Cation Salt Induced C_{sp3}–H Functionalization of Glycine Derivatives: Synthesis of Substituted Quinolines. *Org. Lett.* **2012**, *14*, 4030–4033. (c) Huo, C.; Chen, F.; Yuan, Y.; Xie, H.; Wang, Y. Iron Catalyzed Dual-Oxidative Dehydrogenative (DOD) Tandem Annulation of Glycine Derivatives with Tetrahydrofurans. *Org. Lett.* **2015**, *17*, 5028–5031. (d) Jia, X.; Zhu, Y.; Yuan, Y.; Zhang, X.; Lu, S.; Zhang, L.; Luo, L. C–H Activation Relay (CHAR): An Efficient Construction of Isatin Skeleton by Aerobic Oxidation of Glycine Esters. *ACS Catal.* **2016**, *6*, 6033–6036. (e) Xie, Z.; Jia, J.; Liu, X.; Liu, L. Copper(II) Triflate-Catalyzed Aerobic Oxidative C–H Functionalization of Glycine Derivatives with Olefins and Organoboranes. *Adv. Synth. Catal.* **2016**, *358*, 919–925. (f) Jia, X.; Hou, W.; Shao, Y.; Yuan, Y.; Chen, Q.; Li, P.; Liu, X.; Ji, H. A Consecutive C−H Functionalization Triggered by Oxidation of Active sp^3 C−H Bonds: Construction of 3,4-Dihydroquinoline-3-one Derivatives. *Chem. -Eur. J.* **2017**, *23*, 12980–12984. (g) Li, H. T.; Huang, S. H.; Wang, Y. J.; Huo, C. D. Oxidative Dehydrogenative [2 + 3]-Cyclization of Glycine Esters with Aziridines Leading to Imidazolidines. *Org. Lett*. **2018**, *20*, 92–95. (h) Xie, J. L.; Huang, Y. Q.; Song, H. J.; Liu, Y. X.; Wang, Q. M. Copper-Catalyzed Aerobic Oxidative [2 + 3] Cyclization/Aromatization Cascade Reaction: Atom-Economical Access to Tetrasubstituted 4,5-Biscarbonyl Imidazoles. *Org. Lett.* **2017**, *19*, 6056−6059. (i) Li, Y. J.; Li, X.; Zhang, S. X.; Zhao, Y. L.; Liu, Q. Copper(II)-Catalyzed Oxidative [3+2] Cycloaddition Reactions of Secondary Amines with α-Diazo Compounds: A Facile and Efficient Synthesis of 1,2,3-Triazoles. *Chem. Commun*. **2015**, *51*, 11564–11567.

(15) (a) Narayanam, J. M. R.; Stephenson, C. R. J. Visible Light Photoredox Catalysis: Applications in Organic Synthesis. *Chem. Soc. Rev.* **2011**, *40*, 102–113. (b) Shi, L.; Xia, W. Photoredox Functionalization of C–H Bonds

Adjacent to A nitrogen Atom. *Chem. Soc. Rev.* **2012**, *41*, 7687–7697. (c) Xuan, J.; Xiao, W.-J. Visible-Light Photoredox Catalysis. *Angew. Chem. Int. Ed.* **2012**, *51*, 6828–6838. (d) Prier, C. K.; Rankic, D. A.; MacMillan, D. W. C. Visible Light Photoredox Catalysis with Transition Metal Complexes: Applications in Organic Synthesis. *Chem. Rev.* **2013**, *113,* 5322–5363. (e) Corrigan, N.; Shanmugam, S.; Xu, J.; Boyer, C. Photocatalysis in Organic and Polymer Synthesis. *Chem. Soc. Rev.* **2016**, *45*, 6165–6212. (f) Karkas, M. D.; Porco, J. A.; Stephenson, C. R. J. Photochemical Approaches to Complex Chemotypes: Applications in Natural Product Synthesis. *Chem. Rev*. **2016**, *116*, 9683–9747. (g) Ravelli, D.; Protti, S.; Fagnoni, M. Carbon–Carbon Bond Forming Reactions via Photogenerated Intermediates. *Chem. Rev.* **2016**, *116*, 9850–9913. (h) Romero, N. A.; Nicewicz, D. A. Organic Photoredox Catalysis. *Chem. Rev*. **2016**, *116*, 10075–10166.

(16) For selected examples, see: (a) Condie, A. G.; Gonzalez-Gomez, J. C.; Stephenson, C. R. J. Visible-Light Photoredox Catalysis: Aza-Henry Reactions via C−H Functionalization. *J. Am. Chem. Soc.* **2010**, *132*, 1464–1465. (b) Rueping, M.; Vila, C.; Koenigs, R. M.; Poscharny, K.; Fabry, D. C. Dual Catalysis: Combining Photoredox and Lewis Base Catalysis for Direct Mannich Reactions. *Chem. Commun.* **2011**, *47*, 2360–2362. (c) Miyake, Y.; Nakajima, K.; Nishibayashi, Y. Visible-Light-Mediated Utilization of α-Aminoalkyl Radicals: Addition to Electron-Deficient Alkenes Using Photoredox Catalysts. *J. Am. Chem. Soc.* **2012**, *134*, 3338–3341. (d) Liu, Q.; Li, Y.-N.; Zhang, H.-H.; Chen, B.; Tung, C.-H.; Wu, L. -Z. Reactivity and Mechanistic Insight into Visible-Light-Induced Aerobic Cross-Dehydrogenative Coupling Reaction by Organophotocatalysts. *Chem. -Eur. J.* **2012**, *18*, 620–627. (e) Meng, Q.-Y.; Zhong, J.-J.; Liu, Q.; Gao, X.-W.; Zhang, H.-H.; Lei, T.; Li, Z.-J.; Feng, K.; Chen, B.; Tung, C.-H.; Wu, L.-Z. A Cascade Cross-Coupling Hydrogen Evolution Reaction by Visible Light Catalysis. *J. Am. Chem. Soc.* **2013**, *135*, 19052–19055. (f) Liu, X.; Ye, X.; Bures, F.; Liu, H.; Jiang, Z. Controllable Chemoselectivity in Visible-Light Photoredox Catalysis: Four Diverse Aerobic Radical Cascade Reactions. *Angew. Chem. Int. Ed.* **2015**, *54*, 11443–11447. (g) Wei, G.; Zhang, C.; Bures, F.; Ye, X.; Tan, C.-H.; Jiang, Z. Enantioselective Aerobic Oxidative C(sp^3)–H Olefination of Amines via Cooperative Photoredox and Asymmetric Catalysis. *ACS Catal.* **2016**, *6*, 3708–3712. (h) Yang, Q.; Zhang, L.; Ye, C.; Luo, S.; Wu, L.-Z.; Tung, C.-H. Visible-Light-Promoted Asymmetric Cross-Dehydrogenative Coupling of Tertiary Amines to Ketones by Synergistic Multiple Catalysis. *Angew. Chem. Int. Ed.* **2017**, *56*, 3694–3698. (i) Niu, L. B.; Wang, S. C.; Liu, J. M.; Yi, H.; Liang, X. A.; Liu, T. Y.; Lei, A. W. Visible Light-Mediated Oxidative C(sp^3)–H Phosphonylation for α-Aminophosphonates under Oxidant-Free Conditions. *Chem. Commun*. **2018**, *54*, 1659–1662.

(17) (a) Wang, Z.-Q.; Hu, M.; Huang, X.-C.; Gong, L.-B.; Xie, Y.-X.; Li, J.-H. Direct α-Arylation of α-Amino Carbonyl Compounds with Indoles Using Visible Light Photoredox Catalysis. *J. Org. Chem.* **2012**, *77*, 8705–8711.

(b) Zhu, S.; Rueping, M. Merging Visible-Light Photoredox and Lewis Acid Catalysis for the Functionalization and Arylation of Glycine Derivatives and Peptides. *Chem. Commun.* **2012**, *48*, 11960–11962. (c) Gao, X.-W.; Meng, Q.-Y.; Xiang, M.; Chen, B.; Feng, K.; Tung, C.-H.; Wu, L.-Z. Combining Visible Light Catalysis and Transition Metal Catalysis for the Alkylation of Secondary Amines. *Adv. Synth. Catal.* **2013**, *355*, 2158–2164. (d) Chen, L.; Chao, C. S.; Pan, Y.; Dong, S.; Teo, Y. C.; Wang, J.; Tan, C.-H. Amphiphilic Methyleneamino Synthon through Organic Dye Catalyzed-Decarboxylative Aminoalkylation. *Org. Biomol. Chem.* **2013**, *11*, 5922–5925. (e) Gao, X.-W.; Meng, Q.-Y.; Li, J.-X.; Zhong, J.-J.; Lei, T.; Li, X.-B.; Tung, C.-H.; Wu, L.-Z. Visible Light Catalysis Assisted Site-Specific Functionalization of Amino Acid Derivatives by C–H Bond Activation without Oxidant: Cross-Coupling Hydrogen Evolution Reaction. *ACS Catal.* **2015**, *5*, 2391–2396. (f) Tan, Y.; Yuan, W.; Gong, L.; Meggers, E. Aerobic Asymmetric Dehydrogenative Cross-Coupling between Two C_{sp2}-H Groups Catalyzed by a Chiral-at-Metal Rhodium Complex. *Angew. Chem. Int. Ed.* **2015**, *54*, 13045–13048. (g) Dong, W.; Hu, B.; Gao, X.; Li, Y.; Xie, X.; Zhang, Z. Visible-Light-Induced Photocatalytic Aerobic Oxidation/Povarov Cyclization Reaction: Synthesis of Substituted Quinoline-Fused Lactones. *J. Org. Chem.* **2016**, *81*, 8770–8776. (h) He, Y.-H.; Xiang, Y.; Yang, D.-C.; Guan, Z. Combining Enzyme and Photoredox Catalysis for Aminoalkylation of Indoles via A relay Catalysis Strategy in One Pot. *Green Chem.* **2016**, *18*, 5325–5330. (i) Wang, C.; Guo, M. Z.; Qi, R. P.; Shang, Q. Y.; Liu, Q.; Wang, S.; Zhao, L.; Wang, R.; Xu, Z. Q. Visible-Light-Driven, Copper-Catalyzed Decarboxylative C(sp^3)−H Alkylation of Glycine and Peptides. *Angew. Chem. Int. Ed.* **2018**, *57*, 15841–15846.

(18) (a) Yang, X.; Li, L.; Li, Y.; Zhang, Y. Visible-Light-Induced Photocatalytic Aerobic Oxidative C_{sp3}–H Functionalization of Glycine Derivatives: Synthesis of Substituted Quinolines. *J. Org. Chem.* **2016**, *81*, 12433–12442. (b) Zhang, Y.; Yang, X.; Zhou, H.; Li, S.; Zhu, Y.; Li, Y. Visible Light-Induced Aerobic Oxidative Cross-Coupling of Glycine Derivatives with Indoles: A Facile Access to 3,3′-Bisindolylmethanes. *Org. Chem. Front.* **2018**, *5*, 2120–2125. (c) He, Y.; Yan, B.; Tao, H.; Zhang, Y.; Li, Y. Metal-Free Photocatalyzed Aerobic Oxidative C_{sp3}–H Functionalization of Glycine Derivatives: One-Step Generation of Quinoline-Fused Lactones. *Org. Biomol. Chem.* **2018**, *16*, 3816–3823. (d) Zhou, H.; Yang, X.; Li, S.; Zhu, Y.; Li, Y.; Zhang, Y. Visible Light-Induced Aerobic Oxidative Cross-coupling of Glycine Esters with α-Angelicalactone: A Facile Pathway to γ-Lactams. *Org. Biomol. Chem.* **2018**, *16*, 6728–6734. (e) Li, S. L.; Yang, X. R.; Wang, Y. W.; Zhou, H.; Zhang, B. Y.; Huang, G. X.; Zhang, Y.; Li, Y. Visible Light-Induced Aerobic Oxidative C_{sp3}−H Arylation of Glycine Derivatives. *Adv. Synth. Catal.* **2018**, *360*, 4452– 4456. (f) Yang, X.; Zhu, Y.; Xie, Z. X.; Li, Y.; Zhang, Y. Visible-Light-Induced Charge Transfer Enables Csp^3−H Functionalization of Glycine Derivatives: Access to 1,3-Oxazolidines. *Org. Lett*. **2020**, DOI: 10.1021/acs.orglett.0c00234.

(19) CCDC 1888972 (**3aa**) contains the supplementary crystallographic data for this paper. These data can be obtained free of charge from The Cambridge Crystallographic Data Centre via www.ccdc.cam.ac.uk/data_request/cif